Mon. Not. R. Astron. Soc. **000**, 1–8 (2011) Printed 28 January 2013 (MN LaTeX style file v2.2)

arXiv:1106.1439v1 [astro-ph.CO] 7 Jun 2011

Population III stars and the Long Gamma Ray Burst rate

M.A. Campisi[1]*, U. Maio[2], R. Salvaterra[1], B. Ciardi[3]
[1] *Dipartimento di Fisica e Matematica, Universitá dell'Insubria, via Valleggio 7, 22100 Como, Italy*
[2] *Max-Planck-Institut für extraterrestrische Physik, Giessenbachstraße 1, D-85748 Garching bei München, Germany*
[3] *Max-Planck-Institut für Astrophysik Physik, Karl-Schwarzschild-Straße 1, D-85748 Garching bei München, Germany*

Accepted ???. Received ???; in original form ???

ABSTRACT
Because massive, low-metallicity population III (PopIII) stars may produce very powerful long gamma-ray bursts (LGRBs), high-redshift GRB observations could probe the properties of the first stars. We analyze the correlation between early PopIII stars and LGRBs by using cosmological N-body/hydrodynamical simulations, which include detailed chemical evolution, cooling, star formation, feedback effects and the transition between PopIII and more standard population I/II (PopII/I) stars. From the *Swift* observed rate of LGRBs, we estimate the fraction of black holes that will produce a GRB from PopII/I stars to be in the range 0.028$<f_{GRB}<$0.140, depending on the assumed upper metallicity of the progenitor. Assuming that as of today no GRB event has been associated to a PopIII star, we estimate the upper limit for the fraction of LGRBs produced by PopIII stars to be in the range 0.006$<f_{GRB}<$0.022. When we apply a detection threshold compatible with the BAT instrument, we find that the expected fraction of PopIII GRBs (GRB3) is $\sim 10\%$ of the full LGRB population at $z>$6, becoming as high has 40% at $z>$10. Finally, we study the properties of the galaxies hosting our sample of GRB3. We find that the average metallicity of the galaxies hosting a GRB3 is typically higher than the critical metallicity used to select the PopIII stars, due to the efficiency in polluting the gas above such low values. We also find that the highest probability of finding a GRB3 is within galaxies with a stellar mass $<10^7$ M$_\odot$, independently from the redshift.

Key words: gamma-rays: bursts – Population III; method: numerical.

1 INTRODUCTION

Gamma-ray bursts (GRBs) are the most energetic explosions in the Universe (Zhang & Mészáros 2004), offering exciting possibilities to study astrophysics in extreme conditions and up to very high redshift (z), as shown by the detection of GRB 090423 at $z=8.2$ (Salvaterra et al. 2009; Tanvir et al. 2009). According to recent studies and the so called "collapsar model", long GRBs (LGRBs), with durations longer than $2\,\mathrm{sec}$, are linked with the final evolutionary stages of massive stars. In particular, a Wolf-Rayet star can produce a long GRB if its mass loss rate is "small", which is possible only when the stellar metallicity is very low. Indeed, when metallicities are below $\sim 0.1-0.3\,Z_\odot$, the specific angular momentum of the progenitor allows the loss of the hydrogen envelope while preserving the helium core (Woosley & Heger 2006; Fryer et al. 1999). Observations of high-z LGRBs can provide unique information about the first stages of galaxy formation in the early Universe and on the reionization process (McQuinn et al. 2009). Moreover, it has been recently proposed (Mészáros & Rees 2010; Toma et al. 2010; Suwa & Ioka 2011) that also very massive, metal-free first stars, the so-called Population III (PopIII) stars, can produce a LGRB. The rotation rate has as well important implications for the evolution of the star and the possible production of GRBs. Indeed the stars should retain sufficient spin to power the collapsar burst (Bromm & Loeb 2006; Stacy et al. 2011; Chiappini et al. 2011).

Indeed, a recent study by Suwa & Ioka (2011) shows that the jet can potentially break out the stellar surface even if the PopIII star has a massive hydrogen envelope, thanks to the final long-lasting accretion of the envelope itself onto the central black hole (BH). Since GRB luminosity and duration are found to be very sensitive to the core and envelope mass, they are probe of the first luminous objects at the end of the dark ages. Toma et al. (2010) calculated the afterglow spectra of such PopIII GRBs based on the standard external shock model, showing that they could be detectable with the *Swift* BAT/XRT. Anyway, the rate of GRB from PopIII, even if measurable, is very small. Thus, observations of PopIII stars might be possible only with a large area and with the fields of view of future missions (as e.g. the Fermi LAT instruments).

Thus, GRBs associated to PopIII stars should be observable out to redshift ~ 30 (e.g. Ciardi & Loeb 2000; Toma et al. 2010, and references therein) and might represent the most promising way to directly detect the very first stars (Lamb & Reichart 2000; Bromm & Loeb 2002; Salvaterra et al. 2010).

In this paper, we compare the redshift distribution of LGRBs from

---

* E-mail: campisi@dfm.uninsubria.it

© 2011 RAS

PopII/I stars with the one expected by PopIII stars up to high redshift, by using state-of-the-art N-body/hydrodynamical simulations (see Maio 2008; Maio et al. 2010, 2011; Maio & Iannuzzi 2011), including detailed chemical evolution of the Universe, gas cooling, PopIII-to-PopII/I transition, and feedback effects. To select the candidates for LGRBs, we extract the information for the age and metallicity of newly formed stars, and adopt the collapsar model for both PopII/I and PopIII stars. We build three samples of possible progenitors with different metallicity thresholds, and give estimates of the PopIII GRB rate measured by *Swift*. We additionally compute the contribution of the LGRBs from PopIII progenitors with respect to the total LGRBs rate.

The paper is organized as follows: in Sec. 2, we present the N-body/hydrodynamical chemistry simulations used in this work; in Sec. 3, we describe the method for selecting different progenitors of LGRBs; we describe our results in Sec. 4; then, we describe the main properties of the galaxies hosting our LGRBs from PopIII in Sec.5; finally, we discuss results and give our conclusions in Sec. 6.

2 NUMERICAL SIMULATIONS

We perform N-body/hydrodynamical simulations, including cosmological evolution of e^-, H, H^+, H^-, He, He^+, He^{++}, H_2, H_2^+, D, D^+, HD, HeH^+ (Yoshida et al. 2003; Maio et al. 2006, 2007, 2009), PopIII and PopII/I star formation (Tornatore et al. 2007) according to corresponding initial mass functions (IMF), gas cooling from resonant and fine-structure lines (Maio et al. 2007) and feedback effects (Springel & Hernquist 2003). The transition from the PopIII to the PopII/I regime is determined by the underlying metallicity, Z, of the medium, compared to the critical value $Z_{crit} = 10^{-4} Z_\odot$ (see e.g. Schneider et al. 2003; Bromm & Loeb 2003; Schneider et al. 2006, and references therein). If $Z < Z_{crit}$, then a Salpeter PopIII IMF is assumed with mass range between $100\,\mathrm{M}_\odot$ and $500\,\mathrm{M}_\odot$; otherwise, a standard Salpeter IMF is adopted with mass range between $0.1\,\mathrm{M}_\odot$ and $100\,\mathrm{M}_\odot$, and SNII range between $8\,\mathrm{M}_\odot$ and $40\,\mathrm{M}_\odot$ (see Maio et al. 2011; Bromm et al. 2009).

The chemical model follows the detailed stellar evolution of each SPH particle. At every timestep, the abundances of the different species are consistently derived, according to the lifetimes of the stars and the yields in the given mass range[1]. Metal mixing is mimicked by smoothing the metallicities over the SPH kernel. Pollution is driven by wind feedback, which causes metal spreading over scales of several kpc at each epoch (e.g. Maio et al. 2011). We warn the reader, though, that, due to poorly known quantities in stellar evolution modeling, different assumptions can determine variations in the PopIII-SFR estimates of more than one order of magnitude, as already shown in Maio et al. (2010, 2011), and in Maio & Iannuzzi (2011). More specifically, the largest effects are due to the PopIII IMF assumed in the simulations. Many studies suggest the PopIII IMF to be top-heavy, with stellar masses of the order of hundreds solar masses (e.g. Larson 1998; Abel et al. 2002; Yoshida et al. 2004). However, there is also evidence for a more standard, low-mass PopIII IMF, with masses well below $\sim 100\,\mathrm{M}_\odot$ (e.g. Yoshida 2006; Yoshida et al. 2007; Campbell & Lattanzio 2008; Suda & Fujimoto 2010; Greif et al. 2011). The main difference between these two scenarios is the lifetime of the first SN, which is $\sim 10^6\,\mathrm{yr}$ in the former case, and $\sim 10^8\,\mathrm{yr}$ in the latter, and this results in a transition from the PopIII to the PopII/I regime which takes place earlier in the top-heavy IMF scenario (Maio et al. 2010; Maio & Iannuzzi 2011). On the other hand, uncertainties in the critical metallicity for the PopIII/PopII-I transition, Z_{crit}, are not expected to be crucial, since the rapid pollution process boosts metallicities up to $\sim 10^{-3} Z_\odot$ in few 10^7 yr after the first explosions (Maio et al. 2010).

Table 1. Simulation parameters.

Box side [Mpc/*h*]	Gas particle mass [M$_\odot$/*h*]	Dark matter particle mass[M$_\odot$/*h*]	Maximum physical softening [kpc/*h*]
100	3×10^8	2×10^9	7.50
10	3×10^5	2×10^6	0.50
5	4×10^4	3×10^5	0.25

In the simulation used here, the cosmological field is sampled at redshift $z = 100$, with dark-matter and baryonic-matter species, according to the standard cosmological model, with total-matter density parameter at the present $\Omega_{0,m} = 0.3$, cosmological constant density parameter $\Omega_{0,\Lambda} = 0.7$, baryonic-matter density parameter $\Omega_{0,b} = 0.04$, expansion rate in units of 100 km/s/Mpc $h = 0.7$, spectral normalization $\sigma_8 = 0.9$, and primordial spectral index $n = 1$. We consider three cubic volumes with comoving sides of 100 Mpc/*h*, 10 Mpc/*h*, and 5 Mpc/*h*, with corresponding gas mass resolution of $\sim 3 \times 10^8\,\mathrm{M}_\odot/h$, $\sim 3 \times 10^5\,\mathrm{M}_\odot/h$, $\sim 4 \times 10^4\,\mathrm{M}_\odot/h$, and dark-matter resolution of $\sim 2 \times 10^9\,\mathrm{M}_\odot/h$, $\sim 2 \times 10^6\,\mathrm{M}_\odot/h$, $\sim 3 \times 10^5\,\mathrm{M}_\odot/h$.

The identification of the simulated objects (with their gaseous, dark and stellar components) was carried out by applying a friends-of-friends technique, with comoving linking length of 20% the mean inter-particle separation, and a minimum number of 32 particles. Substructures are identified by using a SubFind algorithm, which discriminates among bound and non-bound particles. The parameters used in the simulations are listed in Table 1.

We show the analysis of the simulation outputs by reconstructing the evolution of the star formation rates (SFRs) in our simulations and comparing with observed data in Fig.1. We find that the total SFR of our larger simulation is in good agreement with the observational data, while the smaller boxes were not evolved below $z \sim 5$ because at these redshifts most of the power in structure formation is at larger scales. Nevertheless, we see that the total SFR converges at $z \sim 5$. In addition, the general trend is very similar, with the contribution from PopIII rapidly decreasing with redshift and reaching $\sim 10^{-4}$ the total SFR. Because of the higher resolution obtained, differently from the 100 Mpc/h box, within the two smaller boxes, we marginally resolve the formation of minihalos. Such primordial objects have typical masses below $\sim 10^8\,\mathrm{M}_\odot$ and as small as $\sim 10^5\,\mathrm{M}_\odot$ and they witness the formation of the first stars. As detailed e.g. in Tornatore et al. (2007) and Maio et al. (2010), the first PopIII stars form in these small mass halos, of pristine composition, and their subsequent formation history depends on the details of metal enrichment and chemical feedback. For this

---

[1] Lifetimes are from Padovani & Matteucci (1993) (but see also, e.g. Maeder & Meynet 1988). The yields used are from Woosley & Weaver (1995) for SNII, van den Hoek & Groenewegen (1997) for AGB stars, Thielemann et al. (2003) for SNIa, Heger & Woosley (2002) for PISN. For a more extensive and detailed discussion on different IMFs and metal yields and their effect on the enrichment history, see also Maio et al. (2010) (in particular Fig. 6 and Fig. 7), and Maio & Iannuzzi (2011)(e.g. Fig. 5).

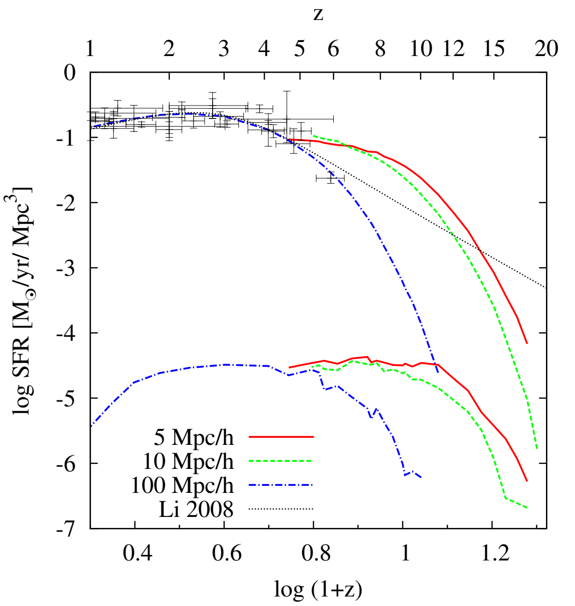

Figure 1. Star formation rate density, $SFR\,[\mathrm{M_\odot\,yr^{-1}\,Mpc^{-3}}]$, as a function of redshift for the simulation with comoving side box of 5 Mpc/h (red-solid line), 10 Mpc/h (green-dashed line) and 100 Mpc/h (blue-dotted-dashes line) . For each of them, we show the total star formation rate density (upper lines) and the SFR of particles with $Z < Z_{crit}$ (PopIII SFRs), i.e. that will produce a GRB3 (lower lines). Symbols with error bars are a compilation of observational data (Hopkins and Beacon 2006), the black-dotted line is the best fit for observational data (Li 2008b).

reasons the smaller boxes are better suited to capture the star formation process at high redshift, when, according to the standard hierarchical scenario of structure formation, the galaxy population is dominated by objects with masses much smaller than the present ones.

3 DIFFERENT PROGENITORS FOR GRBS

We divide the possible progenitors in three subsamples: two associated with PopII stars ($Z > Z_{crit}$), with different upper cuts in metallicity, and one from PopIII stars ($Z \leqslant Z_{crit}$). As mentioned in Sec. 1, recent studies on the final evolutionary stages of massive stars suggest that a Wolf-Rayet star can produce a LGRB if its mass loss rate is small. This is possible only if the metallicity of the star is low, and therefore the specific angular momentum of the progenitor allows the loss of the hydrogen envelope while preserving the helium core (Woosley & Heger 2006; Fryer et al. 1999). The loss of the envelope reduces the material that the jet needs to cross in order to escape, while the helium core should be massive enough to collapse and power a GRB.

In order to select possible progenitors for LGRBs, we have extracted from the simulations the information about the age and the metallicity of all the star particles. In particular, the metallicity is computed as the ratio between the total mass of metals contained in star particles and the total stellar mass. According to the collapsar model, we consider young star particles with age $t < t_c = 5 \times 10^7\,\mathrm{yr}$ (Lapi et al. 2008; Nuza et al. 2007). We follow an approach similar to Campisi et al. (2009), and we will refer to our subsample in the following way:

- GRB1, obtained by selecting star particles associated with PopII/I stars ($Z > Z_{crit}$), without upper metallicity cut;
- GRB2, including star particles associated with PopII/I stars ($Z > Z_{crit}$), and with metallicity $Z \leqslant 0.5 Z_\odot$;
- GRB3, defined by selecting star particles with metallicity $Z \leqslant Z_{crit}$.

In particular, for the second subsample we adopt a metallicity cut of $\sim 0.5\,Z_\odot$ because stronger metallicity cuts seem to be excluded by the analyses of the properties of observed GRB host galaxies at $z < 1$ (Mannucci et al. 2010; Campisi et al. 2011).

In the following, we will briefly describe how we compute the rate of LGRBs (Sec. 3.1), considering both PopII/I (Sec. 3.2) and PopIII (Sec. 3.3) progenitors.

3.1 LGRBs rate

The formation rate of LGRBs in the simulations can be computed by:

$$\rho_{GRB,i}(z) = f_{GRB,i}\ \zeta_{BH,i}\ \rho_{*,i}(z) \qquad (1)$$

where i indicates the 3 subsamples previously described, $f_{GRB,i}$ is the fraction of BHs that will produce a LGRB, $\zeta_{BH,i}$ is the fraction of BHs formed per unit stellar mass, and $\rho_{*,i}(z)$ is the star formation rate for the considered subsample, i.

The observed rate (in units of [yr^{-1} sr^{-1}]) of LGRBs of the i-th subsample at redshift larger than z is then given by

$$\begin{aligned} R_{GRB,i}(>z) &= \gamma_b \int_z dz' \frac{dV(z')}{dz'} \frac{1}{4\pi} \frac{\rho_{GRB,i}(z')}{1+z'} \\ &\times \int_{L_{th}(z')} dL' \psi_i(L'), \qquad (2) \end{aligned}$$

where γ_b is the beaming fraction, $dV(z)/dz$ is the comoving volume element, and ψ_i is the normalized LGRB luminosity function (LF). The factor $(1+z)^{-1}$ accounts for the cosmological time dilation. The last integral gives the fraction of LGRBs with isotropic equivalent peak luminosities $L > L_{th}$, i.e. those LGRBs that can be actually detected by the satellite. The threshold luminosity L_{th} is obtained by imposing a 1-s peak photon flux limit of $P = 0.4$ ph s^{-1} cm^{-2} in the 15-150 keV band of *Swift*/BAT.

There is a general consensus that GRBs are jetted sources (Waxman et al. 1998; Rhoads 1997) implying fundamental corrections to their energy budget and GRB rates. We take into account this fact by considering that the observed LGRB rates should be corrected by the factor γ_b that is related to the jet opening angle θ by $\gamma_b = (1 - \cos\,\theta) \sim \theta^2/2$ (Sari et al. 1998). Given the average value of $\theta \sim 6^\circ$ (Ghirlanda et al. 2007), $<\gamma_b>\sim 5.5 \times 10^{-3}$, which is the value we adopt.

Finally, in order to compute the observed rate we have to specify the LF of LGRB, $\psi_i(L)$, for the three LGRB subsamples considered here. Although the number of LGRBs with good redshift determination has been largely increased by *Swift*, the sample is still too poor (and bias dominated) to allow a direct measurement of the LF. However, an estimate of the LGRB LF and of its evolution through cosmic times can be obtained by fitting the BATSE differential number counts and imposing the constraint on the bursts observed by *Swift* (e.g. Salvaterra & Chincarini (2007); Salvaterra et al. (2009); Campisi et al. (2010), but see Butler et al. (2010); Wanderman & Piran (2010) for different approaches).

In particular, for GRB1-2 subsamples we adopt the LF obtained by Campisi et al. (2010), who described the LF as

$$\psi(L) \propto \left(\frac{L}{L_*}\right)^{\xi} \exp\left(-\frac{L_*}{L}\right), \qquad (3)$$

Table 2. Fraction of BHs that will produce GRB_i, f_{GRBi}. For i =1,2 two different values for the minimum stellar mass to die as a BH are considered. For i=3 two different values for the number of GRBs observed by *Swift*, $N_{GRB_{Swift}}$, are used to constrain f_{GRB3} . See text for details.

f_{GRB_i}	from BHs with $M > 20M_\odot$	from BHs with $M > 40M_\odot$
f_{GRB1}	~ 0.028	~ 0.089
f_{GRB2}	~ 0.044	~ 0.140
	$N_{GRB_{Swift}}$	
	500 (up)	140 (up2)
f_{GRB3}	~ 0.006	~ 0.022

where ξ is the bright-end power index and L_* is a characteristic cut-off luminosity. In order to take into account possible evolution of the LGRB LF, the cut-off luminosity can be written as $L_* = L_0(1+z)^\sigma$ where L_0 is the cut-off luminosity at $z = 0$. Since the SFR evolution of our GRB1 and GRB2 samples are similar to the Host1 sample in Campisi et al. (2010), we adopt here for both subsamples the following value for the LF free parameters: $L_0 = 0.3 \times 10^{50}$ erg s^{-1}, $\sigma = 2$ and $\xi = -1.7$, that provide a good description of the available data. For GRB3, we assume that the LGRB from PopIII stars are expected to be much brighter than PopII/I LGRB. Since typical luminosities should exceed $10^{53.6}$ erg s^{-1} (Toma et al. 2010), we adopt $L_* = 10^{54}$ erg s^{-1} constant in redshift and $\xi \sim -1.7$. However, we consider a range of possible values with $L_* = 10^{53} - 10^{55}$ erg s^{-1} and $-1.5 < \xi < -2.0$. We will discuss the dependences of our results on these parameters in Sec. 4.

3.2 LGRBs from PopII/I stars

The LGRB formation rate (see definition in Eq. 1) can be obtained from the star formation rate in the i-th subsample once $\zeta_{BH,i}$ and $f_{GRB,i}$ have been specified. The fraction of BHs formed per unit stellar mass can be computed by $\zeta_{BH,i} = \int_{m_{min}}^{100} \phi(m_*)dm_*/\int_{0.1}^{100} m_*\phi(m_*)dm_*$ where $\phi(m_*)$ is the Salpeter IMF and m_{min} is the minimum stellar mass of stars dying as BHs. Given the uncertainties on m_{min} we will consider here two cases with $m_{min} = 20\,\mathrm{M}_\odot$ and $m_{min} = 40\,\mathrm{M}_\odot$, the latter consistent with the value assumed in the numerical simulations.

Since not every BHs produces a LGRB, as described in eq. 1, we need to know the efficiency with which this happens, $f_{GRB,i}$. This can be estimated by considering the observed rate of LGRBs detected by *Swift*. Indeed, as of today the *Swift* rate of LGRBs with redshift $z > 1$ is about[2] 57 yr^{-1} sr^{-1}. By imposing this value, we find $f_{GRB,1}$ =0.028 (0.089) and $f_{GRB,2}$ =0.044 (0.140), assuming $m_{min} = 20\,\mathrm{M}_\odot$ ($m_{min} = 40\,\mathrm{M}_\odot$). These values correspond to having ~ 7 (~ 11) LGRBs every 1000 SNe for the GRB1 (GRB2) subsample. We point out here that to compute the $f_{GRB,i}$, we use the simulation with box sizes 100 Mpc/h, since this is the one reaching lower redshifts. We then assume the same value of $f_{GRB,i}$ also for the other simulations. The adopted values are summarized in Table 2.

3.3 LGRBs from PopIII

In a similar way, we have to specify the value of $\zeta_{BH,3}$ and $f_{GRB,3}$ for GRB3. As already mentioned, the first stars have been assumed to be very massive, with masses $>$ 100 M$_\odot$. Stars with masses between $140 - 260$ M$_\odot$ are expected to die as pair-instability supernovae (Heger & Woosley 2002; Zeldovich & Novikov 1971, 1999), leaving no compact remnant.

Thus, only progenitors with masses in the range $100 - 140\mathrm{M}_\odot$ and $260 - 500\mathrm{M}_\odot$ will lead to the formation of a BH possibly triggering a LGRB event. For the assumed PopIII IMF we obtain $\zeta_{BH,3}$ ~0.0032.

The fraction of PopIII stars that will produce LGRBs is unknown. As of today, there is no strong evidence favoring the detection with *Swift* (or any other satellite) of a LGRB associated to a PopIII star. Indeed, even the most distant LGRB detected so far shares common prompt emission and afterglow properties with the low- and intermediate-z LGRB population (Salvaterra et al. 2009), suggesting that it likely originates from a normal PopII progenitor. Thus, we can set a firm upper limit on the fraction of PopIII stars triggering the LGRB event by imposing that no LGRB associated with a PopIII star has been detected by *Swift*[3], that is:

$$\frac{R_{\rm GRB3}(>0)}{R_{\rm GRB}(>0)} < \frac{1}{N_{Swift}}, \qquad (4)$$

where N_{Swift} is the number of LGRBs observed by *Swift*. Thus an upper limit can be set by considering no PopIII LGRB in the whole sample of *Swift* bursts. At the time of writing this consists in 500, corresponding to $f_{\rm GRB3_{up}} = 0.006$. A more gentle constraint can be obtain by considering that some PopIII LGRB can be hidden among those *Swift* bursts without redshift measurement. In this case, $f_{\rm GRB3_{up2}} = 0.022$ is obtained by imposing no PopIII GRB present among the 140 LGRBs with measured z (Table 2). These values correspond to have 1 GRB3 every $< 2(7) \times 10^5\,M_\odot(Z < Z_{crit})$ produced. We note that a part of the high-z GRBs population might be missed by current follow up observations, as about 20% of all bursts appear as "dark", possibly hiding some high-z GRBs. However, there is increasing observational evidence that most GRBs are "dark" because of dust extinction (Cenko et al. 2009; Greiner et al. 2011).

4 RESULTS

The redshift distributions of LGRBs of different subsamples obtained by integrating eq. 2 are shown in Fig. 2. Here we plot the evolution with redshift of observed cumulative rate for our subsamples of LGRBs in simulations with different box size. Dashed-red lines represent the rate of GRB1 ($R_{\rm GRB1}$), while dashed-dotted-blue lines the rate of GRB2 ($R_{\rm GRB2}$). Note that the different choice of the minimum mass of the BHs does not alter the redshift evolution of LGRBs. The solid-dark line is the upper limit for $R_{\rm GRB3}$ case, obtained using $f_{\rm GRB3_{up2}}$, and dotted-line is the rate for the same sample computed using $f_{\rm GRB3_{up}}$. We use the arrows to point out that the computed rate of GRB3 are upper limits. In the bottom panel of each plot we report the ratio between the rate of GRB3 and the total rate, i.e. the sum of the rate of PopII/I GRBs and PopIII GRBs. The solid line refers to the case in which LGRB from

---

[2] Here, we assume that the fraction of LGRBs observed at redshift < 1 is $\sim 20\%$ of the whole sample of bursts, as estimated in Campisi et al. (2010).

[3] Since the simulations stops at $z = 1$, when calculating $R_{\rm GRB3}(>0)$ we assume that the SFR from PopIII stars is negligible at $z < 1$.

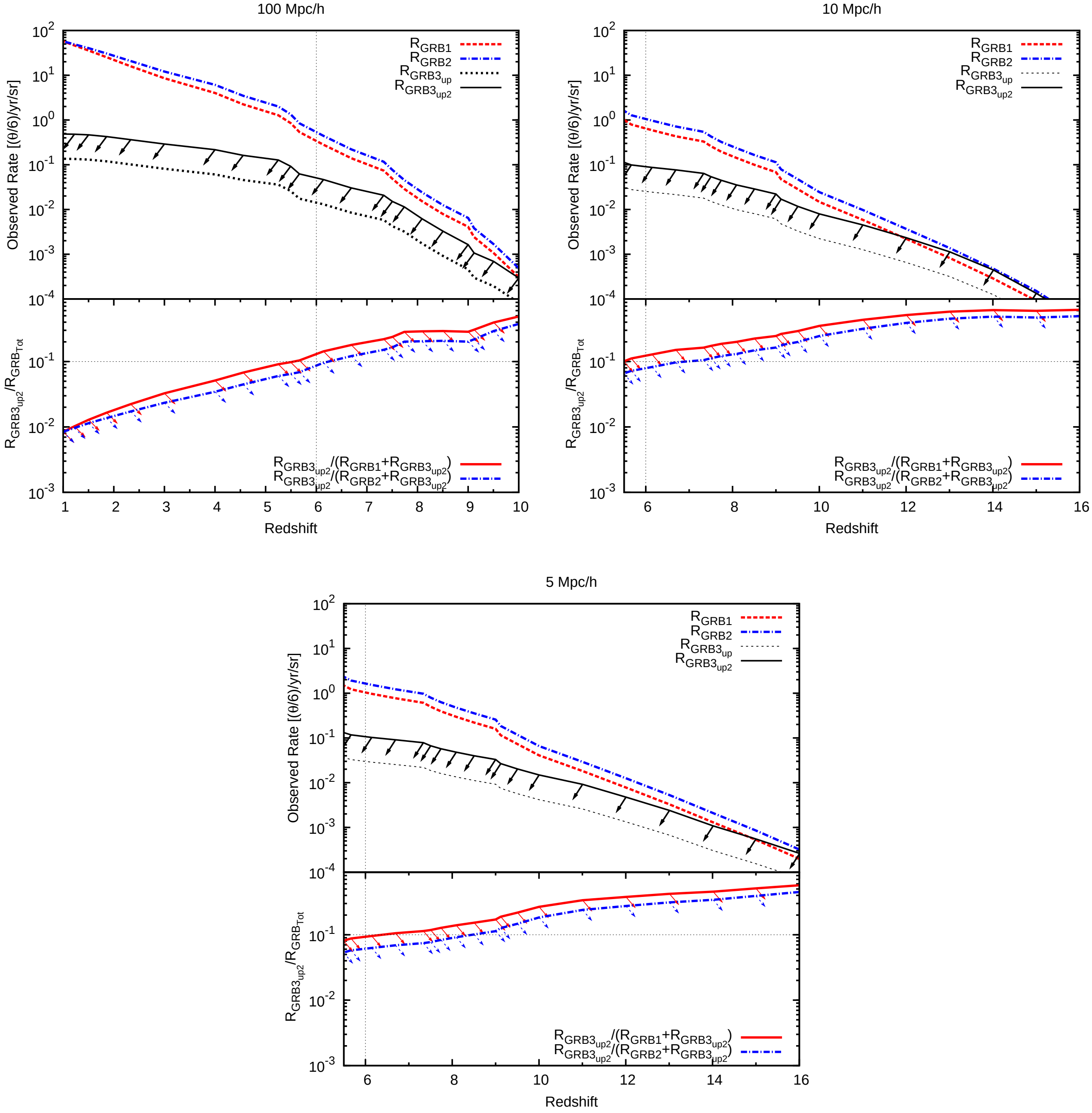

Figure 2. *Top Panels*: Observed rate for our samples of LGRBs in the three simulations with different side box. Dashed-red lines represent the rate of GRB1, dashed-dotted-blue lines the rate of GRB2, the solid-dark lines are the upper limits for the rate of GRB3 and dotted lines are the more restrict upper limit for the same sample (using $f_{\rm GRB3_{up}}$ and $f_{\rm GRB3_{up2}}$ respectively). *Bottom Panels*: Evolution with redshift of the ratio between the expected rate of GRB3 and the total rate obtained summing the rate of the samples GRB3+GRB1 (upper solid-red line) and GRB3+GRB2 (lower dashed-dotted-blue line), for the three simulations with different size box.

PopII/I stars comes from GRB1 subsample whereas dot-dashed line to GRB2 subsample. Here we assume $f_{\rm GRB3_{up2}}$.

If we consider the total rate of LGRB for the 100 Mpc/h simulation, i.e. including the contribution from both PopII/I and PopIII stars, the expected observed rate at redshift z >6 is about $R_{\rm tot}(z>6) \sim 1\,(\theta/6)^2/{\rm yr}/{\rm sr}$. This is consistent with recent observational constraints (Perley et al. 2009; Greiner et al. 2011), as well as with previous theoretical estimates (Salvaterra & Chincarini 2007; Salvaterra et al. 2009; Butler et al. 2010). At these redshifts, the corresponding rate of GRB3 is below 0.017 (0.06) sr^{-1} yr^{-1} for $f_{\rm GRB3_{up}}$ ($f_{\rm GRB3_{up2}}$), and is consistent with Salvaterra et al. (2010) when the same value of $f_{\rm GRB3}$ is adopted. At $z > 6$ the expected fraction of PopIII LGRBs is $\leqslant 10\%$ and increases with redshift. However, at $z \sim 8$ it can not be larger than 20%. This is in agreement with a PopII progenitor for GRB 090423 (Salvaterra et al. 2009; Chandra et al. 2010).

To extend our results to very high z we turn now to our smaller box simulations. Indeed, as already discussed in Sec. 2, at these redshifts the cosmic SFR is dominated by low-mass objects that can be properly resolved only by our small-box simulations. We note that at $z \sim 5-6$ the results of the smaller simulations converge and are in good agreement with those obtained from the 100 Mpc/h side box run. As expected, the contribution of PopIII GRBs is more and more important as redshift increases, becoming dominant for $z > 16$. Thus, a LGRB detected at extremely high redshift would likely be originated from a PopIII star.

These results are not very sensitive on the assumed LF for PopIII LGRB. In fact, we find that the rate of PopIII LGRBs at $z > 6$ is within a factor of two if we vary the characteristic burst luminosity in the range $10^{53} - 10^{55}$ erg s^{-1} and the slope in the range $-1.5 < \xi < -2.0$.

5 HOST GALAXIES OF GRB3 SAMPLE

In Sec. 2 we describe how the host galaxies are obtained from the simulations. The number of expected LGRBs from PopIII in the k-th galaxy can be computed as $N_{k,3} = f_{GRB,3}\ \zeta_{BH,3}\ M_{*,3,k}(z)$, where $M_{*,3,k}$ is the stellar mass in the k-th galaxy that satisfies our selection criteria for the 3-rd subsample (see Sec. 3). Here we are interested in characterizing the properties of PopIII GRB hosts at high z. To this end, we consider the results obtained in the 10 Mpc/h side box run (this choice is motivated by the fact that we need to resolve properly the PopIII hosts and to have sufficient statistics to compute average quantities). We then calculate the probability of having a GRB3 in a host galaxy of a given stellar mass, M_*, and metallicity, Z, in different redshift bins.

In Fig. 3 we show this probability, weighted for the total number of LGRBs, present in the full galaxy sample. Most of the simulated GRB3 hosts are expected to be found in a very well defined region of the $M_* - Z$ plane. These galaxies have always values of Z lower than the solar metallicity at all redshift, but typically higher than the critical value used to select PopIII stars ($Z_{crit} = 10^{-4}\ Z_\odot$). This is because metal enrichment from massive primordial stars proceeds rapidly, and, as soon as they form within a galaxy, they quickly pollute the surrounding environment to values above Z_{crit} (see e.g. Wise & Abel 2008; Greif et al. 2010; Maio et al. 2010, 2011; Maio & Iannuzzi 2011). Despite this, pockets of metal free gas are found within metal enriched galaxies (see e.g. Tornatore et al. 2007), where PopIII star formation can occurr. The details, though, depend on the underlying model of metal enrichment and on the level of turbulent mixing which cannot be properly resolved by cosmological simulations.

GRB3 also seem to reside typically in objects at the lower end of the stellar mass distribution, $M_* \sim 10^5$ M$_\odot$, because these have a higher probability of hosting non polluted gas. On the other hand, they should rarely be found in objects with $M_* > 10^7$ M$_\odot$. It should be noted that this result may depend on the resolution of the simulation. We expect in fact, the typical stellar mass of the host galaxy to decrease when minihalos are properly resolved.

6 DISCUSSIONS AND CONCLUSIONS

LGRBs are now detected up to extreme high redshift and are considered promising tool to study the state of the Universe during and beyond the reionization epoch. Moreover, it has been recently argued that even very massive, metal-free first stars could in principle trigger a LGRB event (Woosley & Heger 2006; Fryer et al. 1999). Given the expected relation between LGRB properties and the BH mass, PopIII LGRBs are predicted to be very bright and detectable with current and future instrument up to $z > 20$ (Bromm & Loeb 2006; Naoz & Bromberg 2007; Toma et al. 2010). If this is the case, the detection of PopIII LGRBs might represent the most promising way to directly probe the nature of the very first stars (Salvaterra et al. 2010).

In this work, we have used three N-body/hydrodynamical cosmological simulations, with various box sizes (L=100 Mpc/h - 10 Mpc/h - 5Mpc/h), to constrain the number and redshift distribution of PopIII LGRBs and compare them to those of PopII/I LGRBs. To estimate the rate of LGRBs of various populations, we assume the collapsar model, and construct three samples of LGRBs: GRB1 are bursts produced by PopII/I stars, GRB2 produced by PopII/I stars with metallicity $Z < 0.5 Z_\odot$ and GRB3 from PopIII stars ($Z < 10^{-4}\ Z_\odot$). In order to compute the rate of PopII/I LGRBs at high z, we follow an observationally motivated approach, by adopting a LGRB luminosity function able to reproduce both the BATSE differential number counts and the redshift distribution of LGRBs detected by *Swift* (Campisi et al. 2010). We find that ~ 1 yr^{-1} sr^{-1} PopII/I LGRBs are predicted to lie at $z > 6$, consistently with available observational constrains (Perley et al. 2009; Greiner et al. 2011) as well as with most recent theoretical works (e.g. Salvaterra et al. 2009; Butler et al. 2010; Wanderman & Piran 2010). In order to constrain the contribution of PopIII LGRBs, we compute an upper limit on the fraction of PopIII stars that can power a LGRB, assuming that none of the bursts detected by *Swift* up-to-now comes from a PopIII progenitor. With this limit, we predict that less than 0.06 sr^{-1} yr^{-1} PopIII LGRBs should be detected at $z > 6$. PopIII LGRBs are found to be non-dominant at $z < 10$ with respect to normal PopII/I LGRBs. However, as expected, their contribution increases with redshift and the probability to find a PopIII LGRBs at $z > 8$ is ∼20%, reaching also $\sim 40-50\%$ at higher redshift, when the contribution of PopIII stars to the total star formation rate is maximum. This implies that if we observed a LGRB at redshift $z > 10$, it would have roughly the same probability to be produced by a PopII/I or PopIII star.

Taking advantage of the detailed description of the simulated galaxies, we further investigate the properties of the possible hosts of PopIII-LGRBs at very-high redshift. We find that the average metallicity of the galaxies hosting a GRB3 is typically higher than the critical metallicity used to select the PopIII stars, due to the efficiency in polluting the gas above such low values. We also find that the highest probability of finding a GRB3 is within galaxies with a stellar mass $< 10^7$ M$_\odot$, independently from the redshift.

They key assumption we have made throughout this paper is that the primordial PopIII IMF is top-heavy with mass range between 100M$_\odot$ and 500M$_\odot$. However, there are many uncertainties about that and different studies (e.g. Yoshida 2006; Yoshida et al. 2007; Campbell & Lattanzio 2008; Suda & Fujimoto 2010) show that smaller-mass first stars could be born even at very early times. This would imply longer stellar lifetimes and two main predictable consequences (see Maio et al. 2010; Maio & Iannuzzi 2011): (i) a general delay in the cosmic enrichment history of roughly $\sim 10^8$ yr; (ii) a larger contribution to the PopIII star formation rate at high redshift.

It is not the aim of the paper to investigate this alternative scenarios, but if this were true, as a consequence we would expect a corresponding increment in the GRB3 rate at high z.

Thanks to the simultaneous observations from the *Swift* and *Fermi* satellites (Bissaldi, E. et al. 2011), future detections of high-z GRBs might help discerning the contribution from PopIII stars, and

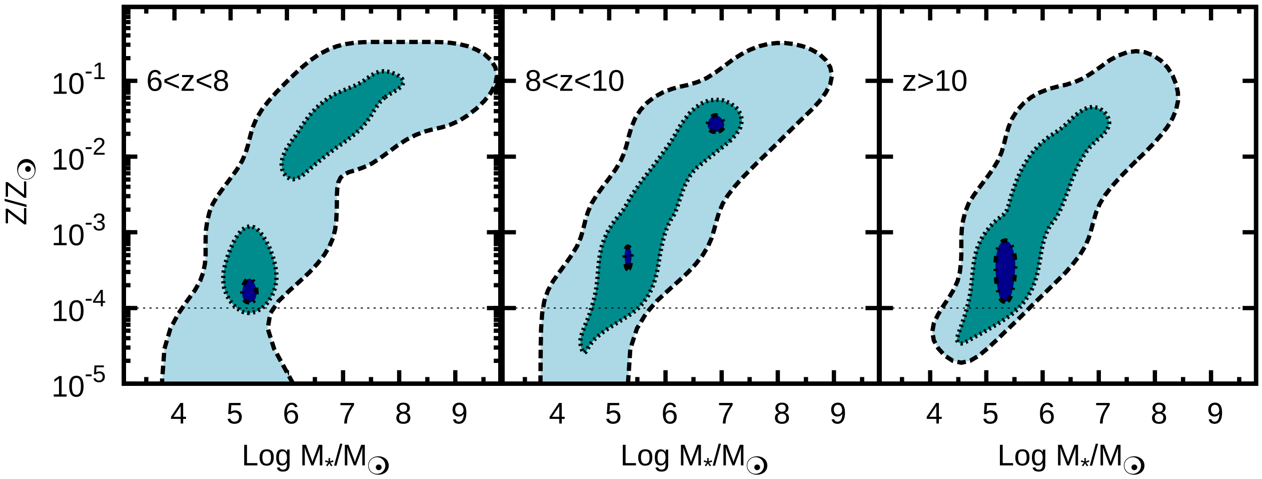

Figure 3. Probability of having a GRB3 in a host galaxy with given stellar mass and metallicity, in three different redshift bins. The contours refer to a probability of 100%, 75% and 25%, where the percentages refer to the contours from the outermost to the innermost, respectively. The horizontal line indicates the critical metallicity Z_{crit}.

if at least 10 GRBs will be detected at $z > 6$ one should be a GRB3. At the present, though, the number of such high-z GRBs is too small and the available data not good enough to discriminate their origin. Nevertheless, the probability of detecting a high-z GRB3 is non-negligible, and it becomes comparable to the probability of detecting a GRB from PopII/I stars at $z > 10$. Thus, investigation of high-z GRBs with future missions (e.g. SWOM, EXIST, ORIGIN, Janus) could offer a realistic first opportunity to detect PopIII stars.

ACKNOWLEDGEMENTS

The authors thank Luca Graziani and Klaus Dolag for important discussions, help and suggestions on numerical aspects of the paper. They also thank the referee, Volker Bromm, for his useful comments which helped improving the presentation of the paper. The simulations and the data analyses were performed on the AMD Opteron machines of the Garching computing center (Rechenzentrum Garching, RZG) of the Max Planck Society. For the bibliographic research we made use of the tools offered by the NASA ADS archive.

REFERENCES

Abel T., Bryan G. L., Norman M. L., 2002, Science, 295, 93
Bissaldi, E. et al. 2011, ApJ, 733, 97
Bromm V., Loeb A., 2002, ApJ, 575, 111
Bromm V., Loeb A., 2003, Nature, 425, 812
Bromm V., Loeb A., 2006, ApJ, 642, 382
Bromm V., Yoshida N., Hernquist L., McKee C. F., 2009, Nature, 459, 49
Butler N. R., Bloom J. S., Poznanski D., 2010, ApJ, 711, 495
Campbell S. W., Lattanzio J. C., 2008, A&A, 490, 769
Campisi M. A., De Lucia G., Li L., Mao S., Kang X., 2009, MNRAS, 400, 1613
Campisi M. A., Li L., Jakobsson P., 2010, MNRAS, 407, 1972
Campisi M. A., Tapparello C., Salvaterra R., Mannucci F., Colpi M., 2011, ArXiv 1105.1378
Cenko S. B., Kelemen J., Harrison F. A., Fox D. B., Kulkarni S. R., Kasliwal M. M., Ofek E. O., Rau A., Gal-Yam A., Frail D. A., Moon D.-S., 2009, ApJ, 693, 1484
Chandra P., Frail D. A., Fox D., Kulkarni S., Berger E., Cenko S. B., Bock D., Harrison F., Kasliwal M., 2010, ApJ, 712, L31
Chiappini C., Frischknecht U., Meynet G., Hirschi R., Barbuy B., Pignatari M., Decressin T., Maeder A., 2011, Nature, 472, 454
Ciardi B., Loeb A., 2000, ApJ, 540, 687
Fryer C. L., Woosley S. E., Hartmann D. H., 1999, ApJ, 526, 152
Ghirlanda G., Nava L., Ghisellini G., Firmani C., 2007, A&A, 466, 127
Greif T., Springel V., White S., Glover S., Clark P., Smith R., Klessen R., Bromm V., 2011, ArXiv e-prints
Greif T. H., Glover S. C. O., Bromm V., Klessen R. S., 2010, ApJ, 716, 510
Greiner J., Krühler T., Klose S., Afonso P., Clemens C., Filgas R., Hartmann D. H., Küpcü Yoldaş A., Nardini M., Olivares E. F., Rau A., Rossi A., Schady P., Updike A., 2011, A&A, 526, A30+
Heger A., Woosley S. E., 2002, ApJ, 567, 532
Lamb D. Q., Reichart D. E., 2000, ApJ, 536, 1
Lapi A., Kawakatu N., Bosnjak Z., Celotti A., Bressan A., Granato G. L., Danese L., 2008, MNRAS, 386, 608
Larson R. B., 1998, MNRAS, 301, 569
Maeder A., Meynet G., 1988, A&A Supp., 76, 411
Maio U., 2008, Dissertation, LMU Munich: Faculty of Physics, pp 1–229
Maio U., Ciardi B., Dolag K., Tornatore L., Khochfar S., 2010, MNRAS, 407, 1003
Maio U., Ciardi B., Yoshida N., Dolag K., Tornatore L., 2009, A&A, 503, 25
Maio U., Dolag K., Ciardi B., Tornatore L., 2007, MNRAS, 379, 963
Maio U., Dolag K., Meneghetti M., Moscardini L., Yoshida N., Baccigalupi C., Bartelmann M., Perrotta F., 2006, MNRAS, 373, 869
Maio U., Iannuzzi F., 2011, MNRAS, in press. ArXiv e-prints: http://adsabs.harvard.edu/abs/2011arXiv1103.3183M
Maio U., Khochfar S., Johnson J. L., Ciardi B., 2011, MNRAS,

pp 397–+
Maio U., Koopmans L. V. E., Ciardi B., 2011, MNRAS, pp L197+
Mannucci F., Salvaterra R., Campisi M. A., 2010, ArXiv e-prints
McQuinn et al. 2009, astro2010: The Astronomy and Astrophysics Decadal Survey, 2010, 199
Mészáros P., Rees M. J., 2010, ApJ, 715, 967
Naoz S., Bromberg O., 2007, MNRAS, 380, 757
Nuza S. E., Tissera P. B., Pellizza L. J., Lambas D. G., Scannapieco C., de Rossi M. E., 2007, MNRAS, 375, 665
Padovani P., Matteucci F., 1993, ApJ, 416, 26
Perley D. A., Cenko S. B., Bloom J. S., Chen H., Butler N. R., Kocevski D., Prochaska J. X., Brodwin M., Glazebrook K., Kasliwal M. M., Kulkarni S. R., Lopez S., Ofek E. O., Pettini M., Soderberg A. M., Starr D., 2009, AJ, 138, 1690
Rhoads J. E., 1997, ApJ, 487, L1+
Salvaterra R., Chincarini G., 2007, ApJ, 656, L49
Salvaterra R., Della Valle M., Campana S., Chincarini G., Covino S., D'Avanzo P., Fernandez-Soto A., Guidorzi C., et al 2009, Nature, 461, 1258
Salvaterra R., Ferrara A., Dayal P., 2010, ArXiv 1003.3873
Salvaterra R., Guidorzi C., Campana S., Chincarini G., Tagliaferri G., 2009, MNRAS, pp 602–+
Sari R., Piran T., Narayan R., 1998, ApJ, 497, L17+
Schneider R., Ferrara A., Salvaterra R., Omukai K., Bromm V., 2003, Nature, 422, 869
Schneider R., Omukai K., Inoue A. K., Ferrara A., 2006, MNRAS, 369, 1437
Springel V., Hernquist L., 2003, MNRAS, 339, 289
Stacy A., Bromm V., Loeb A., 2011, MNRAS, pp 142–+
Suda T., Fujimoto M. Y., 2010, MNRAS, pp 444–+
Suwa Y., Ioka K., 2011, ApJ, 726, 107
Tanvir et al. 2009, Nature, 461, 1254
Thielemann F.-K., Argast D., Brachwitz F., Hix W. R., Höflich P., Liebendörfer M., Martinez-Pinedo G., Mezzacappa A., Panov I., Rauscher T., 2003, Nuclear Physics A, 718, 139
Toma K., Sakamoto T., Meszaros P., 2010, ArXiv e-prints
Tornatore L., Ferrara A., Schneider R., 2007, MNRAS, 382, 945
van den Hoek L. B., Groenewegen M. A. T., 1997, A&A Supp., 123, 305
Wanderman D., Piran T., 2010, MNRAS, 406, 1944
Waxman E., Kulkarni S. R., Frail D. A., 1998, ApJ, 497, 288
Wise J. H., Abel T., 2008, ApJ, 685, 40
Woosley S. E., Heger A., 2006, ApJ, 637, 914
Woosley S. E., Weaver T. A., 1995, ApJS, 101, 181
Yoshida N., 2006, New Astronomy Reviews, 50, 19
Yoshida N., Abel T., Hernquist L., Sugiyama N., 2003, ApJ, 592, 645
Yoshida N., Bromm V., Hernquist L., 2004, ApJ, 605, 579
Yoshida N., Omukai K., Hernquist L., 2007, ApJ, 667, L117
Zeldovich Y. B., Novikov I. D., 1971, Relativistic astrophysics. Vol.1: Stars and relativity. Zeldovich, Y. B. and Novikov,I. D.
Zeldovich Y. B., Novikov I. D., 1999, Stars and relativity. Zeldovich, Y. B. & Novikov, I. D.
Zhang B., Mészáros P., 2004, International Journal of Modern Physics A, 19, 2385